

# Physico-mechanical and Tribological Properties of Fe–Cu–Ni–Sn and Fe–Cu–Ni–Sn–VN Nanocomposites Obtained by Powder Metallurgy Methods

V.A. Mechnik<sup>a</sup>, N.A. Bondarenko<sup>a</sup>, V.M. Kolodnitskyi<sup>a</sup>, V.I. Zakiev<sup>b</sup>, I.M. Zakiev<sup>b</sup>, M. Storchak<sup>c</sup>, S.N. Dub<sup>a</sup>, N.O. Kuzin<sup>d</sup>

<sup>a</sup> V. Bakul Institute for Superhard Materials of the National Academy of Sciences of Ukraine, Kyiv, Ukraine,

<sup>b</sup> National Aviation University, Kyiv, Ukraine,

<sup>c</sup> Institut for Machine Tools, University of Stuttgart, Germany,

<sup>d</sup> Dnipropetrovsk National University of Railway Transport named after Academician V. Lazaryan, Dnipro, Ukraine.

## Keywords:

Composite  
Wear  
Friction coefficient  
Nanohardness  
Elastic modulus.

## ABSTRACT

The results of studies aimed at improving the mechanical and operational properties of the Fe–Cu–Ni–Sn and Fe–Cu–Ni–Sn–VN composite materials obtained by powder metallurgy methods are presented. A comparative analysis of mechanical and tribological characteristics, including the determination of nanohardness, elastic modulus, friction force, friction coefficient, and volume of wear groove was performed. It was shown that the use of 3 wt% nano-dispersed VN powder in the 51Fe–32Cu–9Ni–8Sn charge, in which the grain size was ~2000–5000 nm, makes it possible to increase the nanohardness from 2.68 to 5.37 GPa and reduce the elastic modulus from 199 to 125 GPa. As a result, the parameters  $H/E$  and  $H^3/E^2$ , which describe the resistance of the material to the elastic deformation of failure and the resistance of the material to plastic deformation, increase by 3.3 and 20 times, respectively, and the friction force and the volume of the wear groove decrease by 1.8 and 16 times, respectively. The reasons for the change in the mechanical characteristics of sintered composites during nanoindentation and the different nature of their wear are discussed. The interrelation of the microstructure with mechanical and tribological properties is established. It is shown that the parameters  $H/E$  and  $H^3/E^2$  can be used to predict the wear resistance of the composites under study.

## Corresponding author:

Vasyl Kolodnitskyi  
V. Bakul Institute for Superhard  
Materials of the National Academy  
of Sciences of Ukraine, Kyiv, Ukraine.  
E-mail: [stmj@ism.kiev.ua](mailto:stmj@ism.kiev.ua)

© 2019 Published by Faculty of Engineering

## 1. INTRODUCTION

The development of diamond-containing composites (DCCs) with nanocomposite metal matrices is one of the priorities of modern

materials science. This is due to the fact that the physicomachanical properties of nanocomposite materials are significantly different from the properties of analogs with a coarse-grained structure [1,2]. It is known that the hardness of

Cu-Fe materials with a nanocrystalline structure is 2–7 times higher than that of coarse-grained analogs [3,4]. According to [4], the growth of microhardness in the Cu-Fe nanocomposite is due to the formation of interfaces with an increased dislocation density, since Cu and Fe have different (FCC and BCC) structures. Contrary to the traditional for coarse-grained materials idea of a direct connection of strength and elastic moduli, approaching the nanoscale area of grains in nanostructured materials causes an abrupt decrease in elastic modulus ( $E$ ) and shear coefficient ( $G$ ) while increasing strength and wear resistance [5]. Such effects appear when the average grain size does not exceed 100 nm, and is most clearly observed when the grain size is less than 10 nm [6]. In addition, metal matrix, in contrast to polymer and ceramic, has the best ratio between strength and ductility. Therefore, for a substantial increase in strength and wear resistance, it is important to achieve the maximum possible reduction in the grain size of the matrix during the manufacturing process of DCCs.

Of particular interest are DCCs based on metallic matrices of the Fe-Cu-Ni-Sn system, which are widely used for making tools for the stone-processing industry [7,8]. Many works have been devoted to studying the properties of DCCs with the coarse-grained Fe-Cu-Ni-Sn matrix obtained by powder metallurgy methods. For example, it was established in [9] that the structure of the matrix of the diamond-(Fe-Cu-Ni-Sn) composite obtained by sintering followed by hot addition, regardless of the parameters of hot addition, consists of a solid solution Fe-Cu and  $\text{Cu}_9\text{NiSn}_3$  and  $\text{NiSn}_3$  compounds. While the structure of a transition zone, a diamond-matrix, unlike the structure of a matrix, depends substantially on the parameters of hot re-pressing. It was shown [9] that optimization of the parameters of hot re-pressing enable to form  $\text{Fe}_3\text{C}$  nanoparticles instead of graphite carbon particles in the transition zone. As a result, the wear resistance of the composite increased by 2 times. In [10], a method was developed for calculating the parameters of the structure of the diamond-matrix transition zone, which provides an increase in the tribological properties of the diamond-(Fe-Cu-Ni-Sn) composite obtained by sintering with subsequent hot re-pressing. It was shown that a decrease in the gradient

parameter of the mechanical properties leads to an improvement in the retention of diamond grains by the matrix and an increase in the wear resistance of DCCs. The mechanism for improving the performance properties of these DCCs is the binding of graphite carbon with iron in the form of iron carbide ( $\text{Fe}_3\text{C}$ ). The positive influence of chromium diboride ( $\text{CrB}_2$ ) [11], tungsten carbide (WC) [12], and some nanodispersed additives [13] on the structure and properties of DCCs is known. The influence of the nanocrystalline state on the physicomaterial properties of the Fe-Cu-Ni-Sn matrix has been studied very little and is hardly discussed in the literature. In [14], it was shown that pressing of a Fe-32Cu-9Ni-8Sn (wt%) mixture with the addition of 3 wt% of nanocrystalline vanadium nitride (VN) powder and subsequent hot pressing in vacuum reduced the size of the ferrite grain in the composite from 5–50  $\mu\text{m}$  to 20–400 nm. The structure of the metal matrix consists of a supersaturated solid solution of nitrogen and vanadium in  $\alpha$ -iron, the intermetallic compound  $\text{Cu}_9\text{NiSn}_3$ , and the primary and secondary dispersed phases of VN. All this should lead to an improvement in the mechanical and tribological properties of the matrix, and hence the DCCs.

DCCs metal matrices of tribological purpose should have low abrasive wear, high fatigue strength, as well as high elastic and plastic properties. According to [15], low abrasive wear is usually associated with high hardness, which was also repeatedly observed for DCCs [7, 9–11]. In this regard, when determining the tribological characteristics of DCCs, it should be taken into account that the hardness of the matrix ( $H$ ) is associated with elastic and plastic properties. For most high-volume bulk materials, a large value of the elastic modulus  $E$  is characteristic; therefore, such materials are brittle. However, for many materials, including nanocomposite, it was observed that their wear resistance as well as resistance to elastic deformation of fracture is proportional to  $H/E$  [16,17]. The parameter  $H/E$  is often called the ductility index of the material. To estimate the resistance of a material to plastic deformation using nanoindentation data, the parameter  $H^3/E^2$  is used [18,19]. It follows that in order to increase the resistance of the material to elastic deformation of fracture and reduce plastic deformation; the material must have high hardness with a low modulus of elasticity.

Experimental determinations of the nanohardness  $H$ , elastic modulus  $E$ , parameters  $H/E$  and  $H^3/E^2$ , and also the study of the connection of these parameters with the structure and tribological characteristics of the composites under consideration were not carried out. Moreover, the tribological properties of materials are influenced by strength, load, sliding speed, roughness, coefficient of friction. In the literature, most of these properties are investigated separately from each other and correspond to materials of different nature and structural states. This in turn makes it difficult to perform an analysis of the general or distinctive patterns of the materials in question.

The aim of this paper is to study the mechanical and operational properties of 51Fe–32Cu–9Ni–8Sn and 49.47Fe–31.04Cu–8.73Ni–7.76Sn–3VN (wt%) composites obtained by cold pressing and subsequent sintering in vacuum at temperature 1000 °C pressure 30 MPa for 12 min, and also to establish their connection with the characteristics of the final structure.

## 2. MATERIALS AND RESEARCH METHODS

### 2.1 Materials

Composites with a diameter of 10 mm and a thickness of 8 mm were obtained from a mixture of 51Fe–32Cu–9Ni–8Sn powders (sample 1) and 49.47Fe–31.04Cu–8.73Ni–7.76Sn–3VN (sample 2) (hereinafter mixtures and samples obtained are represented in wt%) by pressing at room temperature and subsequent sintering in vacuum [14]. For the preparation of mixtures, iron, copper, nickel, and tin powders with a grain size of from 5 to 50  $\mu\text{m}$  and vanadium nitride (CAS RN 24646-85-3, "ONYXMET, Poland") with grain sizes from 0.1 to 0.7  $\mu\text{m}$  were used. The mixture of powders was mixed dry in a mixer with an offset axis of rotation for a time 8 h. The pressing the prepared mixtures was carried out at room temperature on a hydraulic press in steel molds at a pressure of 500 MPa. Then, sintering of compacts was carried out in vacuum in graphite molds at a temperature of 1000 °C for 12 min at a final pressure of 30 MPa. For comparison, sample 3 was sintered with a diameter of 10 mm and a thickness of 4 mm from a mixture of 51Fe–32Cu–9Ni–8Sn powders by pressing at room temperature and subsequent

sintering in a hot pre-furnace. The average particle size of the components in this mixture is also 5–50  $\mu\text{m}$ . Sintering of sample 3 was carried out in a steel mold at a temperature of 800 °C for 60 min, followed by hot repressing at a pressure of 160 MPa [10,11].

### 2.2 Micromechanical Characterization

Micromechanical tests were performed on a Nano Indenter II nano-hardness tester from MTS Systems Corporation (USA) with a Berkovich indenter at a load of 5 mN. The growth rate of the load was constant and equal to 0.2 mN/s. The hardness and modulus of elasticity were found by analyzing the indentation unloading curve by the method of Oliver and Pharr [20].

### 2.3 Wear Test

Tribological tests of materials for wear resistance were carried out using pin-on-disk and calo-test methods. Tests using the pin-on-disk method were performed under reciprocating friction (Fig. 1a). A diamond conic indenter with a radius of 50  $\mu\text{m}$  was used as a counterface. To implement the reciprocating movement of the sample, a special additional table was made, which was mounted on a microhardness scratch Micron-gamma tester [21,22]. The Micron-gamma tester is designed to study the micromechanical characteristics of materials using continuous indentation and scratching using different indentation and can detect lateral forces acting on the indenter during loading. The amplitude of the reciprocating motion of the sample relative to the indenter was 2 mm with a load on the indenter of 500 mN and a movement speed of 20 mm/s. The tests were carried out at room temperature.

The calo-test tests with abrasive wear were carried out on a specially made device with a rigidly fixed steel ball on the drive shaft (Fig. 1b). The rigidly fixed ball allows you to control the number of turns without slippage inherent in the traditional calo-test. Friction of a steel ball 2 with a radius of  $R = 10$  mm occurred at a load of  $P = 1$  N with the addition of suspension 1 containing 20 % diamond powder 0.5–1  $\mu\text{m}$  in size. The rotation speed was 72 rpm with duration of 120 s. Abrasive wear resistance was determined by the diameter of the imprint  $D$  of the spherical counterface when it was rubbed over the surface of the sample (see Fig. 1b).

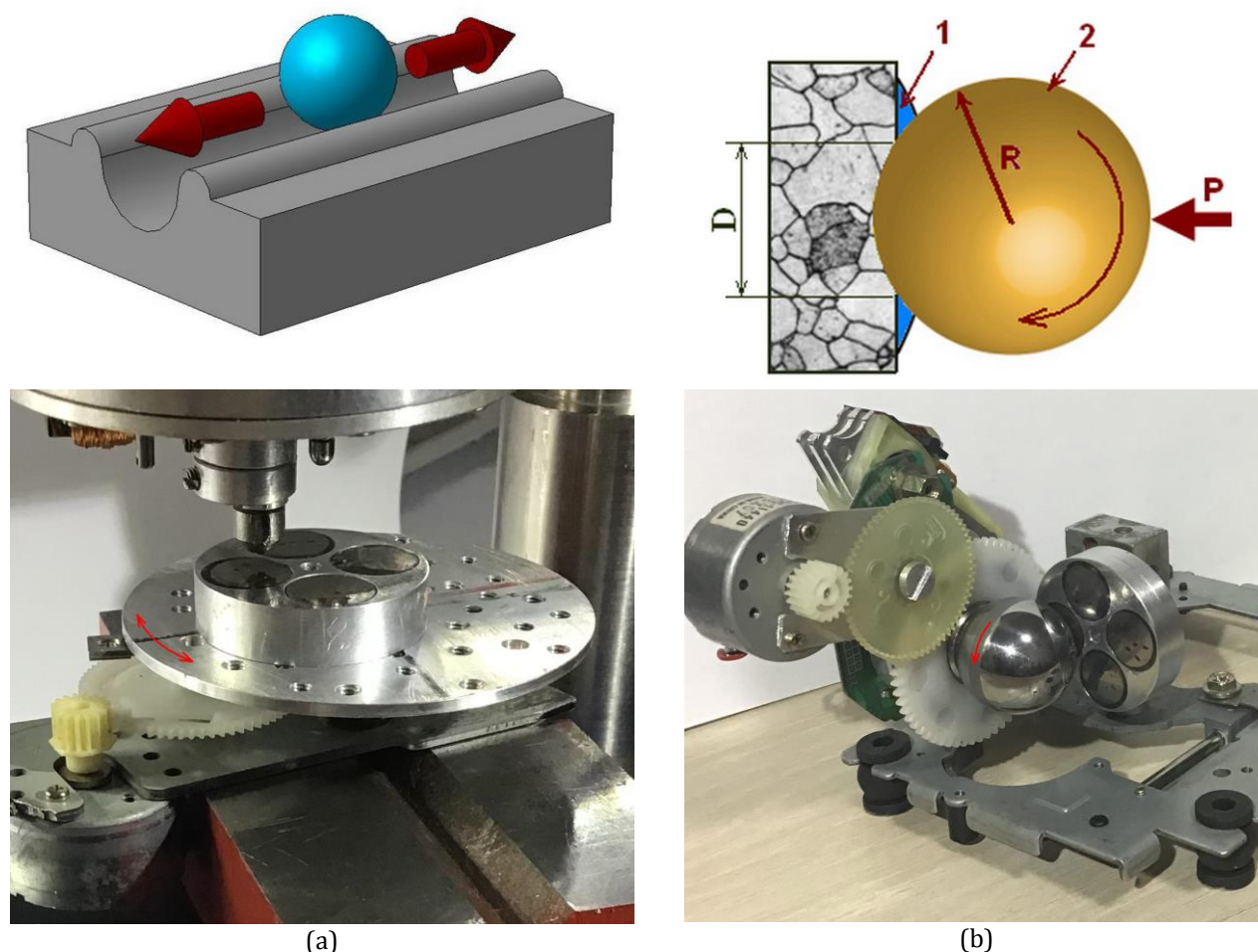


**Fig. 1.** The Models of a Reciprocating Friction by the Pin-on-Disk Method (a) and abrasive Friction by the Calo-Test Method (b) and Photos of Apparatuses, respectively.

The abrasive wear resistance and the volume of the worn crater  $V$  were determined from the diameter of the imprint  $D$  of the spherical counterface when it was rubbed over the surface of the sample (see Fig. 1b). The volume of the wear crater  $V$  was calculated from the condition of equality of the radius of curvature of the crater to the radius of the ball  $R$  by the formula  $V = \pi D^4 / (64R)$ . The wear of the friction tracks was measured on a non-contact interference 3D Micron-alpha profilometer [23], which records surface irregularities with nanometric accuracy.

### 3. RESULTS AND DISCUSSION

#### 3.1 Mechanical properties

The results of the study of nanohardness ( $H$ ), modulus of elasticity ( $E$ ), material resistance to elastic fracture deformation ( $H/E$ ) and resistance of plastic deformation material ( $H^3/E^2$ ) for sintered samples with different dispersion are

given in Table. 1. The Table 1 shows that the mechanical characteristics of the sintered samples vary considerably. In sample 1, the values of  $H$ ,  $E$ ,  $H/E$ , and  $H^3/E^2$  are 4.56 GPa, 191 GPa, 0.024, and 2.60 MPa, respectively. In sample 2, the hardness increases from 4.56 to 5.37 GPa, and the modulus of elasticity decreases from 191 to 125 GPa. At the same time, there is a sharp increase in the  $H/E$  ratio (from 0.024 to 0.043) and  $H^3/E^2$  (from 2.60 to 9.91 GPa). The reason for the increase in  $H$ ,  $H/E$ , and  $H^3/E^2$  and the decrease of  $E$  in sample 2 as compared to sample 1 may be a decrease in grain size and the absence of residual (unconverted) austenite (FCC phase), whose hardness is small.

According to [14], the structure of sample 2 consists of a supersaturated nitrogen and vanadium solid solution in  $\alpha$ -iron (grain size  $\sim 20$ – $400$  nm) and a mixture of nanodispersed VN and  $\text{VO}_2$  phases, which improves the mechanical characteristics. In sample 1, both the BCC of  $\alpha$ -Fe and FCC of  $\gamma$ -Fe phases, as well as the  $\text{Cu}_9\text{NiSn}_3$  phase with larger ( $400$ – $800$  nm) grains were



detected. This in turn impairs the mechanical characteristics and may lead to increased wear [16]. Similar values of  $H$  and  $H/E$  with a low elastic modulus  $E$  ( $\sim 114$  GPa) were also obtained in the study of multicomponent titanium alloys, which are characterized by a nanocrystalline structure [24]. It should be noted that a decrease in the elastic moduli of Cu and Ni by 10–15% was also found in [5]. The lowest values of  $H$  (2.68 GPa),  $H/E$  (0.013), and  $H^3/E^2$  (0.49 GPa) were recorded for sample 3 (Table 1) obtained from the 51Fe–32Cu–9Ni–8Sn mixture by cold pressing and subsequent sintering with hot pressing. The observed deterioration of the mechanical characteristics of this sample is due to the coarse-grained structure and the presence of residual (unconverted) austenite. In this case, the grain size was 2000–5000 nm [9].

From the presented data it is clear that the mechanical properties of the sintered samples are determined by the characteristics of their structure, composition and method of preparation. Sintered sample 1 with a grain size of 400–800 nm has a nanohardness is 1.7 times higher with the same elastic modulus as compared to the coarse-grained sample 3 (grain size  $\sim 2000$ –5000 nm).

A decrease in the size of ferritic grain from 400–800 to 20–400 nm in sample 2 as compared with sample 1 leads to a 1.5-fold decrease in the elastic modulus and an increase in nanohardness from 4.56 to 5.37 GPa. These features lead to a 1.8-fold increase in  $H/E$  and a 3.8-fold increase in  $H^3/E^2$ . The results obtained

indicate that for sample 2 compared with samples 1 and 3, we should expect increased wear resistance. In a number of works, an improvement in the mechanical properties of various materials, including nanocomposite materials, was also observed. For example, in [3], it was shown that the hardness of a composite Cu–Fe system with a nanoscale structure is 2–7 times higher than that of coarse-grained analogs. In [25], it was also shown that the nanostructured alloy Ti–24Nb–4Zn–7.9Sn with a BCC lattice has a sufficiently high hardness and a low modulus of elasticity. A decrease in the elastic moduli of Cu and Ni by 10–15% was also found in [5].

Thus, it was found that with a decrease in the grain size, an improvement in the mechanical characteristics of the sintered composites is observed. At the same time, the resistance of the material to elastic deformation of fracture and the resistance of the material to plastic deformation increase in composites with higher hardness and lower elastic modulus. The most intriguing of the results presented is an indication of the possible greater wear resistance of fine-grained structures compared to coarse-grained ones.

### 3.2. Tribological properties

The dependence of the friction force  $F_{fr}$  on the operating time during the reciprocating movement of the diamond indenter with a radius of curvature 50  $\mu\text{m}$  along the surface of the samples under study is shown in Fig. 2.

**Table 1.** Mechanical Characteristics of sintered Samples.

Sample	Composition	Temperature ( $^{\circ}\text{C}$ )	Grain size (nm)	Nanohardness $H$ (GPa)	Elastic modulus $E$ (GPa)	$H/E$	$H^3/E^2$ (MPa)
1	Fe–Cu–Ni–Sn	1000	400–800	4.56	191	0.024	2.60
2	Fe–Cu–Ni–Sn–VN	1000	20–400	5.37	125	0.043	9.91
3	Fe–Cu–Ni–Sn	800	2000–5000	2.68	199	0.013	0.49

\*Taking into account the relatively small (5–50 nm) [14] grain size of VN, the nanohardness was determined for the iron-containing regions.

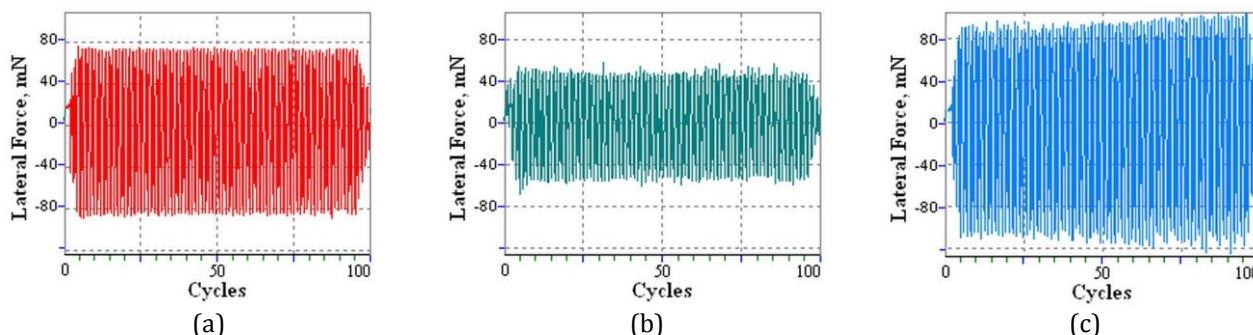


**Fig. 2.** The Dependences of the Friction Force for Samples 1 (a), 2 (b) and 3 (c) on the Number of Reciprocating Movements.

In the study of  $F_{fr}$  on the running time, it was possible to trace the dependence according to which  $F_{fr}$  decreased in accordance with the decrease in the grain size and the improvement of the physico-mechanical properties of the composite. So the average value of  $F_{fr}$  for sample 1, for which the grain size of ~800–400 nm is 76 mN (Fig. 2a), which is less than  $F_{fr}$  (92 mN) for sample 3 (Fig. 4c), for which the grain size ~2000–5000 nm (Table 1). With a further decrease in the grains size (20–400 nm), the average value of  $F_{fr}$  for sample 2 decreased to 50 mN (see Fig. 4b), which is much less than for samples 1 and 3. A characteristic feature of samples 1 and 2 is the fact that with increasing load cycles the friction force  $F_{fr}$  behaves stably (see Fig. 2a and b). While for sample 3 there is a tendency to increase of the friction force (Fig. 2c). It should be noted that an increase in the friction force leads to an increase in the friction coefficient and contact temperature

and, consequently, to an increase in wear. It is possible to note a general pattern inherent in samples 1 and 2, a decrease in the friction force and, as a result, the friction coefficient, due to the formation of a fine-grained structure and the presence of more solid nanodispersed phases [14].

For a qualitative and quantitative assessment of the tribological characteristics of sintered samples at reciprocating friction, two-dimensional topographies with profilograms of cross-sections and three-dimensional images of the areas  $200 \times 130 \mu\text{m}$  of the friction tracks are presented (Fig. 3). A comparative analysis of the topography of the friction tracks showed that for samples 1 and 2 the width (Fig. 3a and c) and depth (Fig. 3b and d) of the wear groove have smaller values than accordingly the width (Fig. 3e) and depth (Fig. 3f) of the grooves for wear for sample 3.

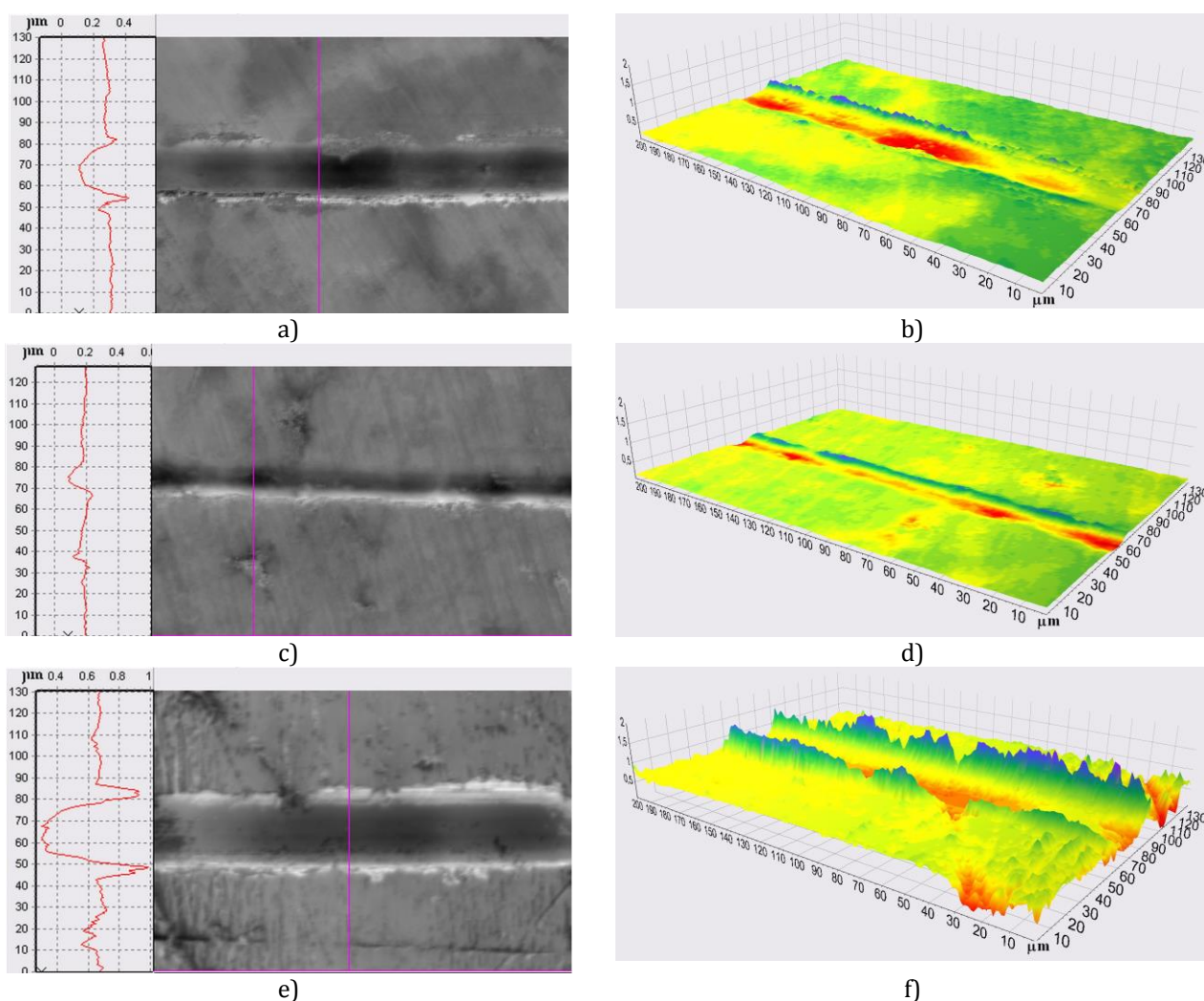


**Fig. 3.** 2-D Topography with Profilograms (a, c, e) and 3-D Images (b, d, f) of  $200 \times 130 \mu\text{m}$  Areas of Friction Tracks of Samples 1 (a, b), 2 (c, d) and 3 (e, f).

The smallest values of the wear groove depth (Fig. 3d) and, as a result, the greatest wear resistance is observed for nanostructured sample 2. For sample 1 with a larger grain size, the wear groove depth has greater value (Fig. 3b) and even more for the coarse-grain sample 3 (Fig. 3f).

Thus, from the data obtained above, it follows that the wear resistance of sintered samples is determined by the grain size of the structural components and the micromechanical characteristics ( $H$ ,  $E$ ,  $H/E$ , and  $H^3/E^2$ ).

In Table 2 presents the results of a study of the average volume of the friction track ( $V$ ) and the friction coefficient ( $\mu$ ) in reciprocating friction. At the same time, wear resistance was estimated by the average volume of friction tracks  $V$ , and the friction coefficient  $\mu$  as the ratio of friction force and normal load ( $F_{fr}/P$ ). From the analysis of the data obtained, it follows that nanostructured sample 2, in

contrast to coarse-grained samples 1 and 3, is characterized by the greatest wear resistance and the lowest coefficient of friction. So the average value of the friction track volume  $V$  for sample 2 is  $3.11 \mu\text{m}^3$ , which is 4 and 16 times less, respectively, than the similar parameter for samples 1 and 3. In this case, the value of the friction coefficient  $\mu$  was 0.1. This is 1.5 and 1.8 times less than for coarse-grained samples 1 and 3, respectively. Sample 2 is the most wear-resistant, whose parameters  $H/E$  and  $H^3/E^2$  have the highest values (see Table 1). This increase is provided by the structure of sample 2, containing the  $\alpha$ -Fe phase with a grain size of 20–400 nm, as well as strengthening nanoscale particles of vanadium nitride (VN) and vanadium oxide ( $\text{VO}_2$ ) [14]. Therefore, the structural features of nanocomposite 2 lead to differences in its physicomechanical and tribological properties from the properties of coarse-grained analogues (samples 1 and 3).

**Table 2.** Tribological and sclerometric characteristics of sintered samples.

Sample	Composition	Friction force $F_{fr}$ (mN)	Volume of friction track $V$ ( $\mu\text{m}^3$ )	Friction coefficient $\mu$
1	Fe–Cu–Ni–Sn	76	12.6	0.152
2	Fe–Cu–Ni–Sn–VN	50	3.11	0.1
3	Fe–Cu–Ni–Sn	92	50.3	0.184

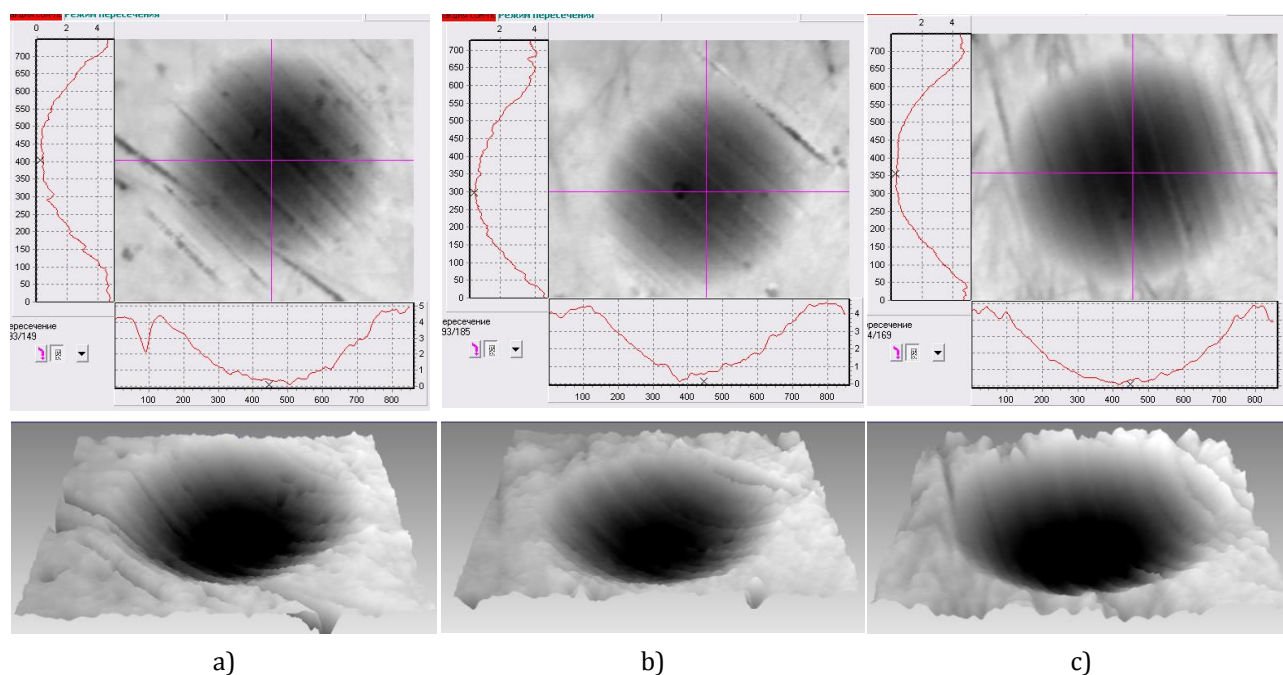


**Fig. 4.** 2-D (upper) and 3-D (lower) Topography of the Wear Craters obtained by the “Calo-Test” Method after Friction of the Surface of the Samples 1 (a), 2 (b) and 3 (c) with a Steel Ball.

**Table 3.** Tribological characteristics of sintered samples obtained by the calo-test method.

Sample	Composition	Diameter of wear crater $D$ ( $\mu\text{m}$ )	Volume of worn material ( $\mu\text{m}^3$ )
1	Fe–Cu–Ni–Sn	2424	169406326
2	Fe–Cu–Ni–Sn–VN	2048	86315504
3	Fe–Cu–Ni–Sn	2919	356406336

Thus, nanostructured sample 2, in contrast to the coarse-grained samples 1 and 3, can significantly improve the mechanical properties, reduce the friction coefficient and significantly increase the wear resistance. This fact indicates the feasibility of its use for the manufacture of DCCs and tools based on them for the stone industry. An increase in the wear resistance of nanostructured metallic materials in comparison with their coarse-grained analogues was also found in other works. Thus, as the nickel grain size decreases from 10,000 nm to 10 nm, the wear rate decreases by more than two orders of magnitude [26]. A comparative analysis of the topography of the friction tracks showed that for samples 1 (Fig. 4a) and 2 (Fig. 4b) the diameter of wear crater and the volume of worn material have smaller values than accordingly similar parameters for sample 3 (Fig. 4c). The smallest values of the diameter of wear crater and the volume of worn material and, as a result, the greatest wear resistance are observed for nanostructured sample 2 (Fig. 4b). The largest values of the diameter of wear crater and the volume of worn material are found for the coarse-grain sample 3 (Fig. 4c).

Indeed, the minimum volume of worn material 86315504  $\mu\text{m}^3$  (Table 3) and, as a consequence, the minimum wear was achieved for nanostructured sample 2 with the highest hardness and lowest elastic modulus equal to 5.37 and 125 GPa, respectively (Table 1). The reduced wear resistance of samples 1 and 3 compared with sample 2 is due to the larger grain size and lower levels of hardness  $H$  and the parameters  $H/E$  and  $H^3/E^2$  (Table 1). The results of tribological tests obtained by the pin-on-disk and calo-test methods correlate well with the results of the physicomechanical properties of sintered composites. From the data obtained, it follows that the wear resistance of the composites under study increases with decreasing grain size and with increasing parameters  $H$ ,  $H/E$ , and  $H^3/E^2$  (Table 1).

The images shown in Fig. 5 are direct evidence of the connection of the microstructure with the mechanical and tribological properties of sintered composites.

In the structure of the sample obtained from the charge with the addition of vanadium nitride, a small grain of ferrite ( $\alpha\text{-Fe}$ ) is formed with a significant variation in size (from 20 to 400 nm) and the intermetallic phases  $\text{Cu}_9\text{NiSn}_3$  ( $\leq 400$  nm) (Fig. 5a). The particle size of vanadium nitride (VN) and vanadium oxide ( $\text{VO}_2$ ) ranges from 5 to 100 nm (Figs. 5a and 5c). Particles of VN sized 50 nm and greater are apparently the primary powder particles. Particles sized up to 10 nm are secondary VN particles released during the decay of a supersaturated nitrogen and vanadium solid solution in  $\alpha$ -iron. Nitrides are located both along the grain boundaries, and per the volume, mainly on dislocations. Inside the largest fragments, one can observe the remains of non-dissolved nitride particles (Fig. 5c). In a sample sintered from a charge without vanadium nitride, a coarse-grained structure with a grain size of 5–40  $\mu\text{m}$  is observed (Figs. 5e and 5f). Sample electron diffraction patterns demonstrate ring reflections from the BCC lattice of  $\alpha\text{-Fe}$  (110), (211), (200), (310), phases of  $\text{Cu}_9\text{NiSn}_3$  (511), (660), VN (220), (200) and  $\text{VO}_2$  (120), (101), (110) (Figs. 5b and 5d). A sharp decrease of the grain size in the sample with the addition of vanadium nitride compared with the sample without vanadium nitride is accompanied by a significant increase in the nanohardness  $H$  from 2.68 to 5.37 GPa, the resistance of the elastic deformation of the fracture  $H/E$  from 0.013 to 0.043, the resistance of the material to plastic deformation  $H^3/E^2$  from 0.49 to 9.91 MPa and wear resistance by 4 times (Table 2 and 3). Thus, the initial the composites microstructure had a significant effect on their mechanical and tribological properties during wear.

Thus, it was found that cold pressing of 51Fe–32Cu–9Ni–8Sn and 49.47Fe–31.04Cu–8.73Ni–7.76Sn–3VN mixtures with a grain size of 2000–5000 nm followed by sintering in vacuum produced nanocomposites with enhanced mechanical and tribological characteristics. High values of the parameters  $H$ ,  $H/E$ , and  $H^3/E^2$  with a relatively low modulus of elasticity are an indicator of high wear resistance of the considered composites. These parameters, in turn, significantly depend on the size effect.



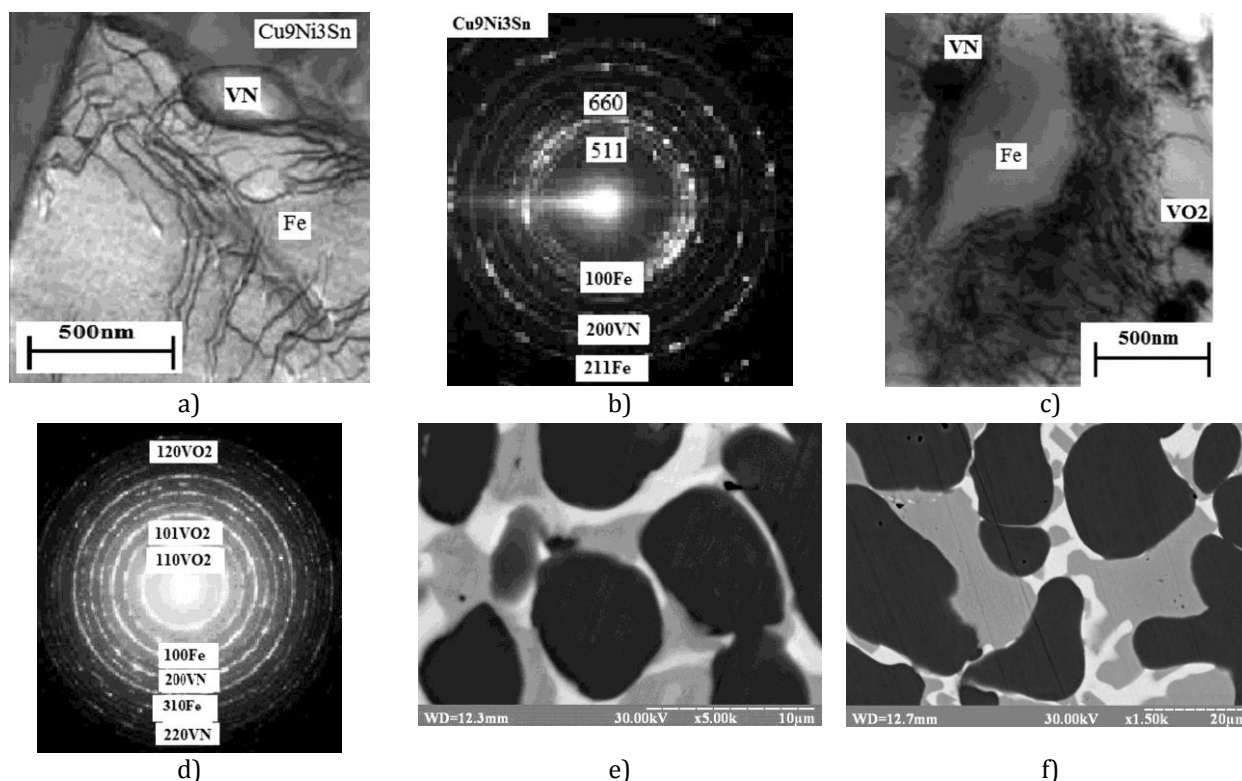


**Fig. 5.** TEM images of the structure (a, c) and the corresponding electron diffraction patterns (b, d) of 49.47Fe–31.04Cu–8.73Ni–7.76Sn–3VN composite and CEM images of the structure 51Fe–32Cu–9Ni–8Sn composite (e, f) [14].

To predict the wear resistance of such composites, you can use the parameters  $H/E$  and  $H^3/E^2$ , which characterize the resistance of the material to elastic deformation of fracture and the resistance of the material to plastic deformation, respectively. The composite of composition 49.47Fe–31.04Cu–8.73Ni–7.76Sn–3VN, whose grain size after sintering is 20–400 nm, is optimal from the point of view of mechanical and tribological characteristics. This composite had the highest  $H$ ,  $H/E$ , and  $H^3/E^2$  and the lowest values of elastic modulus and wear rate. The results can be used to develop of diamond-containing composites as work items in cutting wheels, wire saws and grinding tools for the stone industry.

#### 4. CONCLUSIONS

1. The 51Fe–32Cu–9Ni–8Sn composite, obtained by cold pressing and subsequent sintering in vacuum (sample 1), has a fine-grained structure with a grain size of 400–800 nm and elevated mechanical ( $H = 4.56$  GPa,  $E = 191$  GPa) properties, as well as relatively small values of the friction force ( $F_{fr} = 76$  mN), the wear groove volume ( $V = 12.6 \mu\text{m}^3$ ) and the friction coefficient ( $\mu = 0.152$ ) compared to a similar composite, produced by the method of cold pressing with subsequent sintering with hot re-pressing.
2. The 51Fe–32Cu–9Ni–8Sn composite material strengthened with vanadium nitride nanoparticles in an amount of 3 wt% has a finer-grained structure with a grain size of 20–400 nm and the most balanced mechanical values ( $H = 5.37$  GPa,  $E = 125$  GPa,  $H/E = 0.043$ ,  $H^3/E^2 = 9.91$  MPa) and tribological ( $F_{fr} = 50$  mN,  $V = 3.11 \mu\text{m}^3$ ,  $\mu = 0.1$ ) properties.
3. The improvement of the mechanical and tribological properties of sample 2 compared to sample 1 is due to the formation of a finer-grained microstructure consisting of a supersaturated  $\alpha$ -solid solution (BCC phase of  $\alpha$ -Fe) with a grain size of 20–400 nm, primary and secondary phases of vanadium nitrides with a size grain 5–100 nm.
4. The reason for the sharp decrease in the mechanical and tribological properties of the 51Fe–32Cu–9Ni–8Sn composite (sample 3), obtained by cold pressing and further sintering with hot addition, is the formation of a coarse-grained structure with a grain size of 2000–5000 nm, consisting of  $\alpha$ -Fe,  $\gamma$ -Fe and  $\text{Cu}_9\text{Ni}_3\text{Sn}$  phases.

5. The relationship between the structure, mechanical and tribological properties of composite materials has been established. The greater the  $H$ ,  $H/E$ , and  $H^3/E^2$  and smaller values of  $E$  composite materials, the higher their performance.
6. To predict the wear resistance of the studied composite materials can use the parameters  $H/E$  and  $H^3/E^2$ , describing the resistance of the material to elastic deformation of fracture and the resistance of the material to plastic deformation, respectively.

## Acknowledgements

The work was performed in the framework of state budget research topics in accordance with the coordination plans of the Ministry of Education and Science of Ukraine (state registration number of the project No. 0117U000391).

## REFERENCES

- [1] H. Gleiter, *Nanostructured materials: basic concepts and microstructure*, Acta Mater., vol. 48, pp. 1–29, 2000, doi: [10.1016/S1359-6454\(99\)00285-2](https://doi.org/10.1016/S1359-6454(99)00285-2)
- [2] H. Gleiter, *Materials with ultrafine microstructures: Retrospectives and perspectives*, Nanostructured Mater., vol. 1, pp. 1–19, 1992, doi: [10.1016/0965-9773\(92\)90045-Y](https://doi.org/10.1016/0965-9773(92)90045-Y)
- [3] W.U. Zhiwei, J. Zhang, Yi Chen, M. Liang, *Effect of rare earth addition on microstructural, mechanical and electrical characteristics of Cu–6%Fe microcomposites*, J. Rare Earths, vol. 27, pp. 87–91, 2009, doi: [10.1016/S1002-0721\(08\)60197-0](https://doi.org/10.1016/S1002-0721(08)60197-0)
- [4] L. He, E. Ma, *Processing and microhardness of bulk Cu–Fe nanocomposites*, Nanostruct. Mater., vol. 7, pp. 327–339, 1996, doi: [10.1016/0965-9773\(96\)00003-7](https://doi.org/10.1016/0965-9773(96)00003-7)
- [5] N.A. Akhmadeev, N.P. Kobelev, R.R. Mulyukov, Ya.M. Soifer, R.Z. Valiev, *The effect of heat treatment on the elastic and dissipative properties of copper with the submicrocrystalline structure*, Acta Metall. Mater., vol. 41, 1993, pp. 1041–1046, doi: [10.1016/0956-7151\(93\)90153-J](https://doi.org/10.1016/0956-7151(93)90153-J)
- [6] A.I. Gusev, *Effects of the nanocrystalline state in solids*, Phys. Usp., vol. 41, pp. 49–76, 1998, doi: [10.1070/PU1998v041n01ABEH000329](https://doi.org/10.1070/PU1998v041n01ABEH000329)
- [7] V.A. Mechnyk, *Diamond–Fe–Cu–Ni–Sn composite materials with predictable stable characteristics*, Materials Sci., vol. 48, pp. 591–600, 2013, doi: [10.1007/s11003-013-9542-1](https://doi.org/10.1007/s11003-013-9542-1)
- [8] A.A. Zaitsev, D.A. Sidorenko, E.A. Levashov, V.V. Kurbatkina, S.I. Rupasov, V.A. Andreyev and P.V. Sevast'yanov, *Development and application of the Cu–Ni–Fe–Sn-based dispersion-hardened bond for cutting tools of superhard materials*, J. Superhard Mater., vol. 34, pp. 270–280, 2012, doi: [10.3103/S1063457612040090](https://doi.org/10.3103/S1063457612040090)
- [9] V.A. Mechnik, *Production of diamond–(Fe–Cu–Ni–Sn) composites with high wear resistance*, Powder Metall. Met. Ceram., vol. 52, pp. 577–587, 2014, doi: [10.1007/s11106-014-9563-9](https://doi.org/10.1007/s11106-014-9563-9)
- [10] V.A. Mechnik, N.A. Bondarenko, N.O. Kuzin, B.A. Lyashenko, *The role of structure formation in forming the physicomechanical properties of composites of the diamond–(Fe–Cu–Ni–Sn) system*, J. Frict. Wear, vol. 37, pp. 377–384, 2016, doi: [10.3103/S1068366616040139](https://doi.org/10.3103/S1068366616040139)
- [11] V.A. Mechnik, *Effect of hot recompaction parameters on the structure and properties of diamond–(Fe–Cu–Ni–Sn–CrB<sub>2</sub>) composites*, Powder Metall. Met. Ceram., vol. 52, pp. 709–721, 2014, doi: [10.1007/s11106-014-9579-1](https://doi.org/10.1007/s11106-014-9579-1)
- [12] D.A. Sidorenko, A.A. Zaitsev, A.N. Kirichenko, E.A. Levashov, V.V. Kurbatkina, P.A. Loginov, S.I. Rupasov, V.A. Andreev, *Interaction of diamond grains with nanosized alloying agents in metal–matrix composites as studied by Raman spectroscopy*, Diam. Relat. Mater., vol. 38, pp. 59–62, 2013, doi: [10.1016/j.diamond.2013.05.007](https://doi.org/10.1016/j.diamond.2013.05.007)
- [13] A.A. Zaitsev, D.A. Sidorenko, E.A. Levashov, V.V. Kurbatkina, V.A. Andreev, S.I. Rupasov, P.V. Sevast'yanov, *Diamond tools in metal bonds dispersion-strengthened with nanosized particles for cutting highly reinforced concrete*, J. Superhard Mater., vol. 32, pp. 423–431, 2010, doi: [10.3103/S1063457610060080](https://doi.org/10.3103/S1063457610060080)
- [14] V.A. Mechnik, N.A. Bondarenko, S.N. Dub, V.M. Kolodnitskyi, Yu.V. Nesterenko, N.O. Kuzin, I.M. Zakiev, E.S. Gevorkyan, *A study of microstructure of Fe–Cu–Ni–Sn and Fe–Cu–Ni–Sn–VN metal matrix for diamond containing composites*, Mater. Charact., vol. 146, pp. 209–216, 2018, doi: [10.1016/j.matchar.2018.10.002](https://doi.org/10.1016/j.matchar.2018.10.002)
- [15] E. Rabinowicz, *Friction and Wear of Materials*, New York: John Wiley&Sons, 336 pp., 1995, doi: [10.1115/1.3625110](https://doi.org/10.1115/1.3625110)
- [16] A. Leyland, A. Matthews, *On the significance of the H/E ratio in wear control: a nanocomposite coating approach to optimised tribological*

- behaviour, *Wear*, vol. 246, pp. 1–11, 2000, doi: [10.1016/S0043-1648\(00\)00488-9](https://doi.org/10.1016/S0043-1648(00)00488-9)
- [17] N.V. Novikov, M.A. Voronkin, S.N. Dub, I.N. Lupich, V.G. Malogolovets, B.A. Maslyuk, G.A. Podzyarey, *Transition from polimer-like to diamond-like a-C:H films: Structure and mechanical properties*, *Diam. Relat. Mater.*, vol. 6, pp. 574–578, 1997, doi: [10.1016/S0925-9635\(96\)00642-5](https://doi.org/10.1016/S0925-9635(96)00642-5)
- [18] J. Soldán, J. Musil, *Structure and mechanical properties of DC magnetron sputtered TiC/Cu films*, *Vacuum*, vol. 81, pp. 531–538, 2006, doi: [10.1016/j.vacuum.2006.07.013](https://doi.org/10.1016/j.vacuum.2006.07.013)
- [19] J. Musil, *Tribological and mechanical properties of nanocrystalline-TiC/a-C nanocomposites thin films*, *J. Vac. Sci. Technol. A*, vol. 28, pp. 244–249, 2010, doi: [10.1116/1.3294717](https://doi.org/10.1116/1.3294717)
- [20] W.C. Oliver, G.M. Pharr, *An improved for determining hardness and elastic modulus using load and displacement sensing indentation experiments*, *J. Mater. Res.*, vol. 7, pp. 1564–1583, 1992, doi: [10.1557/JMR.1992.1564](https://doi.org/10.1557/JMR.1992.1564)
- [21] M. Storchak, I. Zakiev, L. Träris, *Mechanical properties of subsurface layers in the machining of the titanium alloy  $Ti_{10}V_2Fe_3Al$* , *J. Mech. Sci. Technol.*, vol. 32, pp. 315–322, 2018, doi: [10.1007/s12206-017-1231-9](https://doi.org/10.1007/s12206-017-1231-9)
- [22] S.R. Ignatovich, I.M. Zakiev, *Universal micronanoindentermeter Micron-gamma*, Industrial Laboratory. Materials Diagnostics, vol. 77, pp. 61–67, 2011.
- [23] V. Zakiev, A. Markovsky, E. Aznakayev, I. Zakiev, E. Gursky, *Micro-mechanical properties of bio-materials*, *Proc. SPIE 5959, Medical Imaging*, 595916 (23 September 2005), Event: Congress on Optics and Optoelectronics, 2005, Warsaw, Poland, doi: [10.1117/12.628396](https://doi.org/10.1117/12.628396)
- [24] S.A. Firstov, V.F. Gorban, N.A. Krapivka, E.P. Pechkovskii, N.I. Danilenko, M.V. Karpets, *Mechanical properties of multicomponent titanium alloy*, *Strength Mater.*, vol. 42, pp. 622–630, 2010, doi: [10.1007/s11223-010-9250-0](https://doi.org/10.1007/s11223-010-9250-0)
- [25] Y.L. Hao, S.J. Li, S.Y. Sun, C.Y. Zheng, R. Vang, *Elastic deformation behaviour of Ti–24Nb–4Zn–7.9Sn for biomedical application*, *Acta Biomaterialia*, vol. 3, pp. 277–286, 2007, doi: [10.1016/j.actbio.2006.11.002](https://doi.org/10.1016/j.actbio.2006.11.002)
- [26] A. Robertson, U. Erb, G. Palumbo, *Practical applications for electrodeposited nanocrystalline materials*, *Nanostructured Mater.*, vol. 12, pp. 1035–1040, 1999, doi: [10.1016/S0965-9773\(99\)00294-9](https://doi.org/10.1016/S0965-9773(99)00294-9)